Figure S1

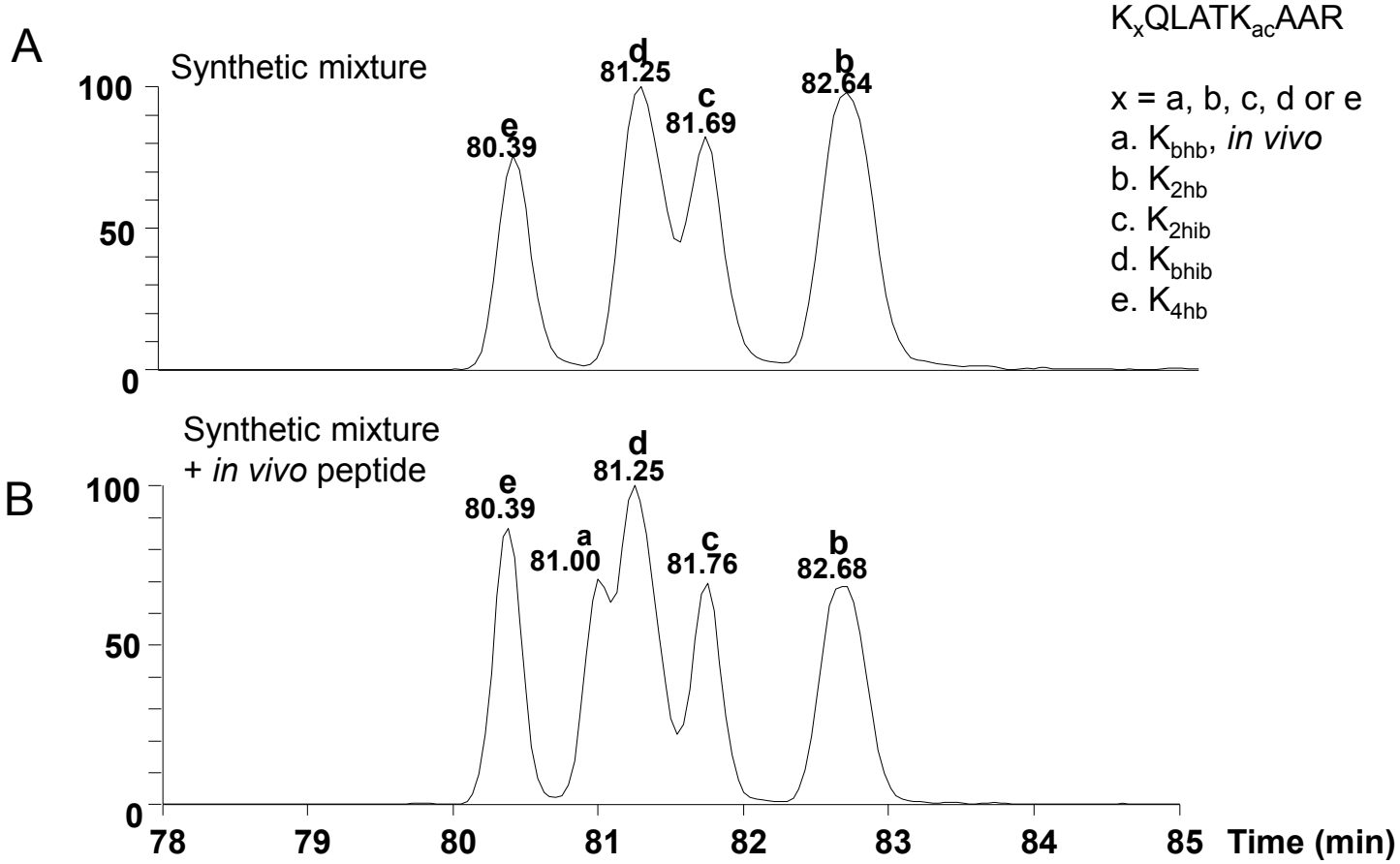
A
Synthetic mixture
$K_xQLATK_{ac}AAR$
x = a, b, c, d or e
a. K_{bhb}, *in vivo*
b. K_{2hb}
c. K_{2hib}
d. K_{bhib}
e. K_{4hb}
e 80.39
d 81.25
c 81.69
b 82.64
B
Synthetic mixture
+ *in vivo* peptide
e 80.39
a 81.00
d 81.25
c 81.76
b 82.68
Time (min)

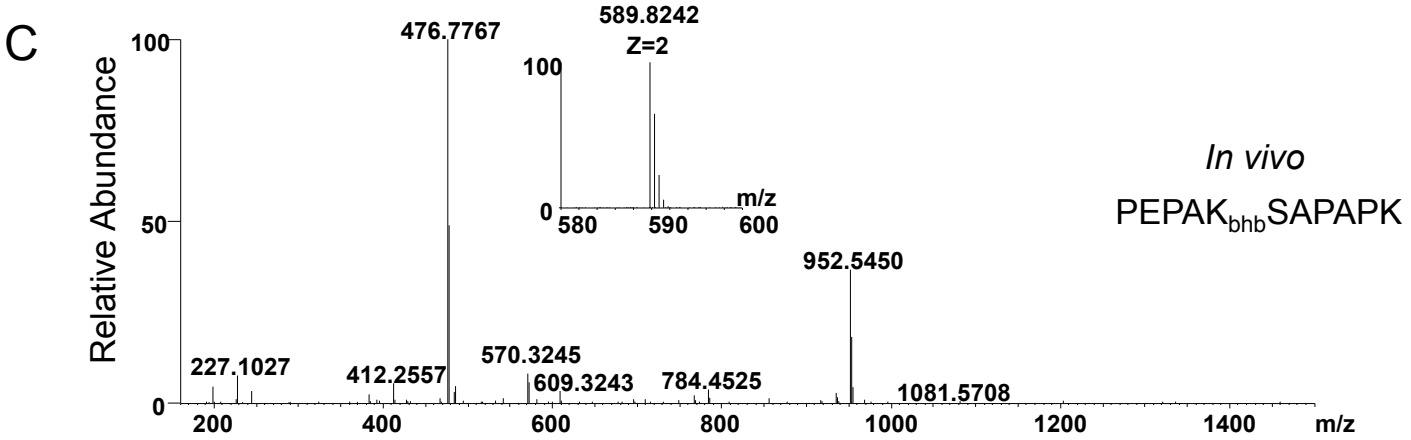
C
Relative Abundance
476.7767
589.8242
Z=2
In vivo
$PEPAK_{bhb}SAPAPK$
952.5450
227.1027
412.2557
570.3245
609.3243
784.4525
1081.5708
m/z

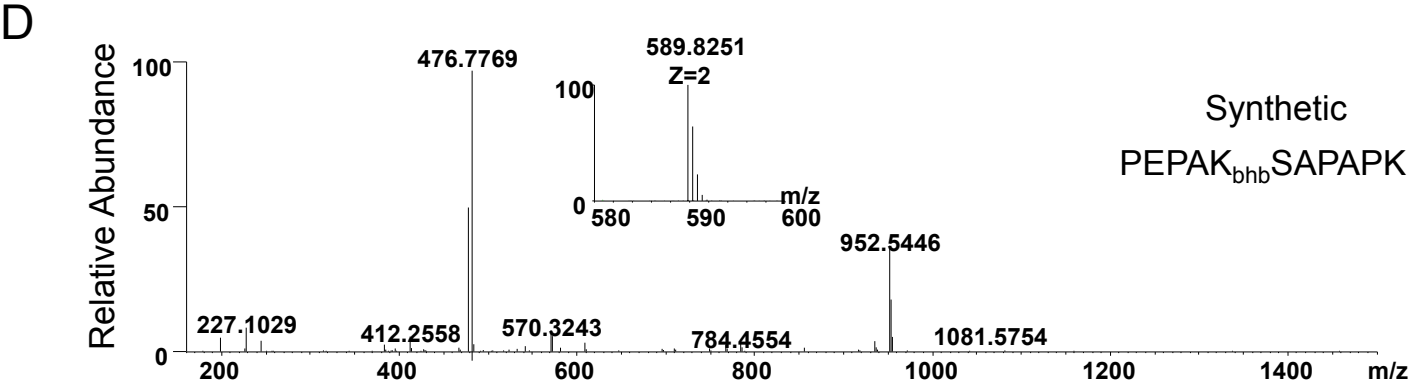
D
Relative Abundance
476.7769
589.8251
Z=2
Synthetic
$PEPAK_{bhb}SAPAPK$
952.5446
227.1029
412.2558
570.3243
784.4554
1081.5754
m/z

Figure S1. Identification and Verification of a Histone Kbhb Peptide, Related to Figure 1.

(A, B) HPLC co-elution experiments for *in vivo* derived K_{bhb}QLATK_{ac}AAR peptide and their structural isomers. (A) Reconstructed ion chromatograms of the mixture of the four synthetic peptides. (B) Reconstructed ion chromatograms of the four synthetic peptides with *in vivo* peptide K_{bhb}QLATK_{ac}AAR obtained from a tryptic digest of histones from HEK293 cells. The x axis represents retention time of HPLC/MS analysis, and the y axis represents the MS signal.

(C, D) MS/MS spectra of the *in vivo*-derived peptide identified from trypsin-digested histones from HEK293 cells (C); and synthetic peptide PEPAK_{bhb}SAPAPK (D). Inserts show the mass-to-charge ratios (m/z) of the precursor peptide ions. The x axis represents m/z and the y axis represents relative ion intensity.

Figure S2

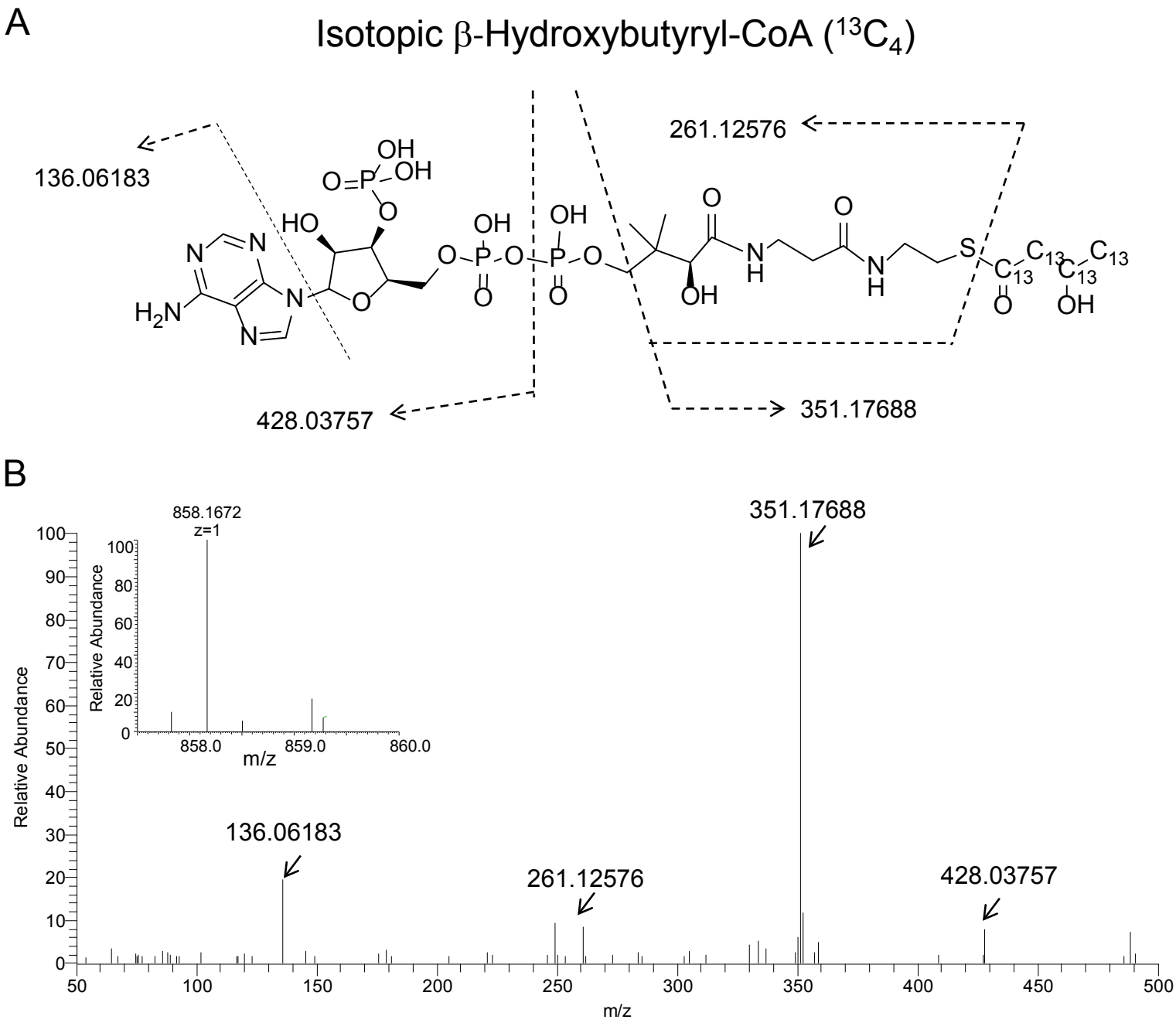
A
Isotopic β-Hydroxybutyryl-CoA ($^{13}C_4$)
136.06183
261.12576
428.03757
351.17688
B
858.1672
z=1
Relative Abundance
m/z
351.17688
136.06183
261.12576
428.03757

Figure S2. MS/MS Measurement of Isotopic β-Hydroxybutyryl-CoA, Related to Figure 2.

(A) Illustration of fragmentation pattern of isotopic β-hydroxybutyryl-CoA ($^{13}C_4$), which is drawn by Chembiodraw 12.0.

(B) MS/MS spectrum of isotopic β-hydroxybutyryl-CoA ($^{13}C_4$) detected from HEK293 cells treated with isotopic sodium β-hydroxybutyrate. The x axis represents m/z and the y axis represents relative ion intensity.

Figure S3

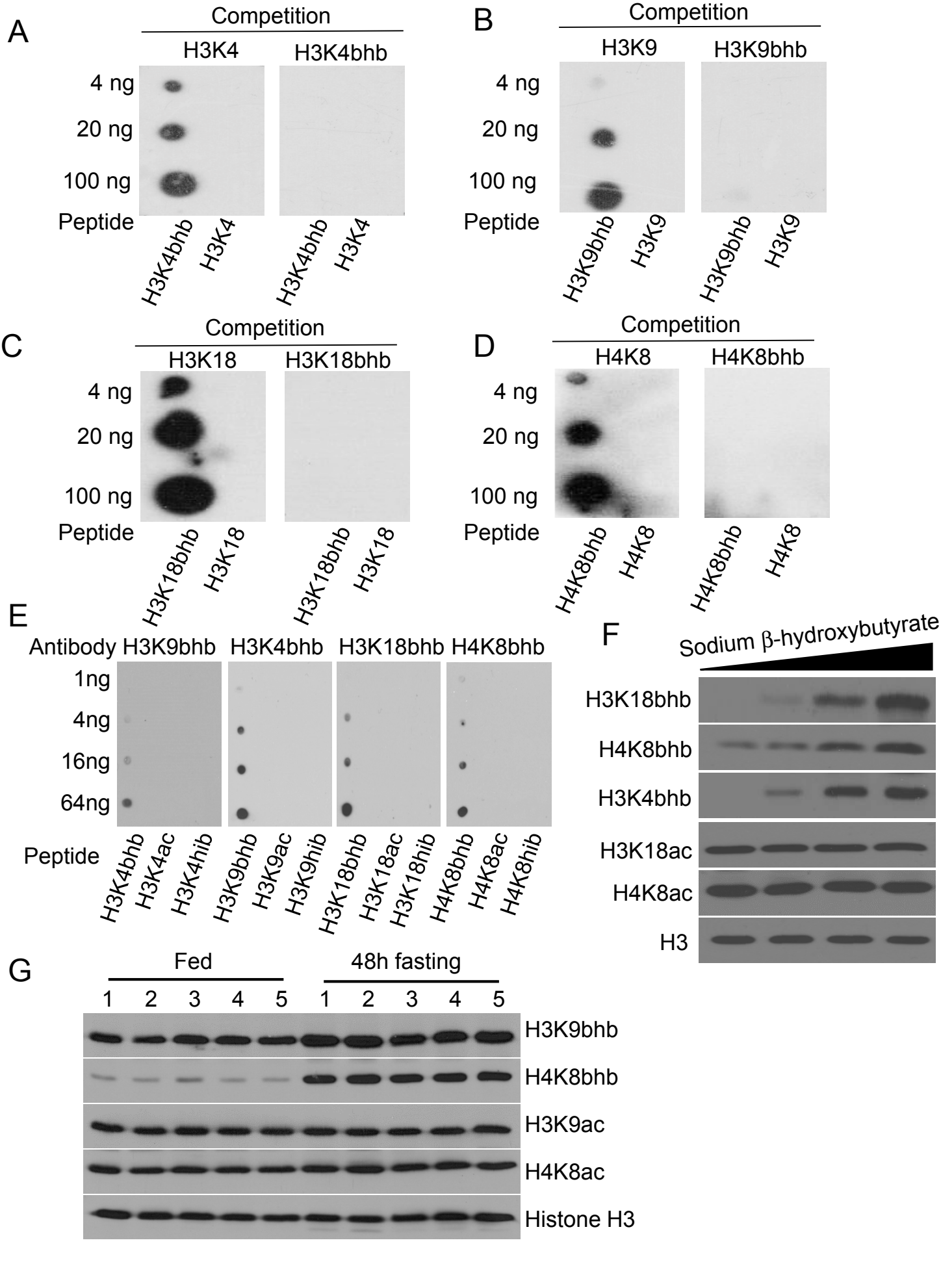
A
Competition
H3K4
H3K4bhb
4 ng
20 ng
100 ng
Peptide
H3K4bhb
H3K4
H3K4bhb
H3K4
B
Competition
H3K9
H3K9bhb
4 ng
20 ng
100 ng
Peptide
H3K9bhb
H3K9
H3K9bhb
H3K9
C
Competition
H3K18
H3K18bhb
4 ng
20 ng
100 ng
Peptide
H3K18bhb
H3K18
H3K18bhb
H3K18
D
Competition
H4K8
H4K8bhb
4 ng
20 ng
100 ng
Peptide
H4K8bhb
H4K8
H4K8bhb
H4K8
E
Antibody H3K9bhb
H3K4bhb
H3K18bhb
H4K8bhb
1ng
4ng
16ng
64ng
Peptide
H3K4bhb
H3K4ac
H3K4hib
H3K9bhb
H3K9ac
H3K9hib
H3K18bhb
H3K18ac
H3K18hib
H4K8bhb
H4K8ac
H4K8hib
F
Sodium β-hydroxybutyrate
H3K18bhb
H4K8bhb
H3K4bhb
H3K18ac
H4K8ac
H3
G
Fed
48h fasting
1 2 3 4 5 1 2 3 4 5
H3K9bhb
H4K8bhb
H3K9ac
H4K8ac
Histone H3

Figure S3. Antibody Specificities for Histone Kbhb and Responses to Sodium β-Hydroxybutyrate Treatment, Related to Figure 3.

(A-E) Specificities of anti-H3K4bhb, anti-H3K9bhb, anti-H3K18bhb, and anti-H4K8bhb antibodies revealed by dot blot and competition assay. Dot-blot assay was carried out using indicated site-specific anti-Kbhb antibody and indicated amount of modified peptides. Bhb represents β-hydroxybutyrylation; ac represents acetylation; hib represents 2-hydroxyisobutyrylation.Competition was carried out by incubation of indicated site-specific anti-Kbhb antibody with 10-fold excess of unmodified or Kbhb containing peptides.

(F) HEK293 cells were untreated or treated with 2mM, 5mM and 10mM of sodium β-hydroxybutyrate respectively. Histones were acid extracted and immunoblotted by the indicated antibodies.

(G) Dynamics of histone Kbhb and Kac during 48h of starvation in kidney.

Figure S4

A

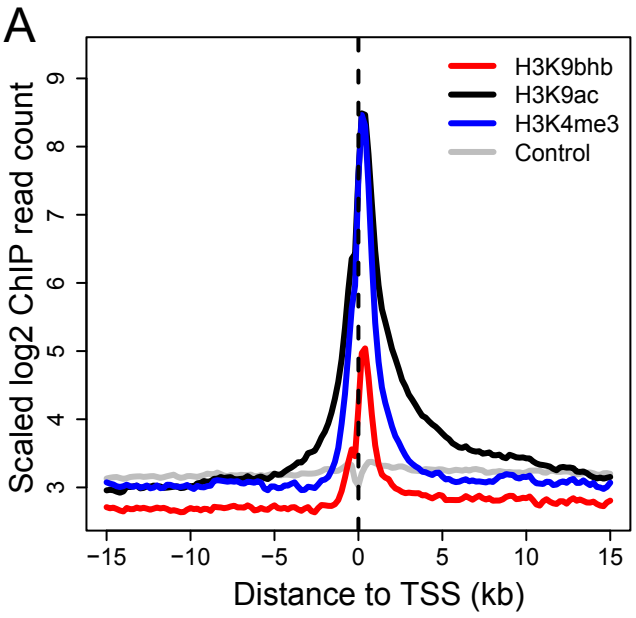

B

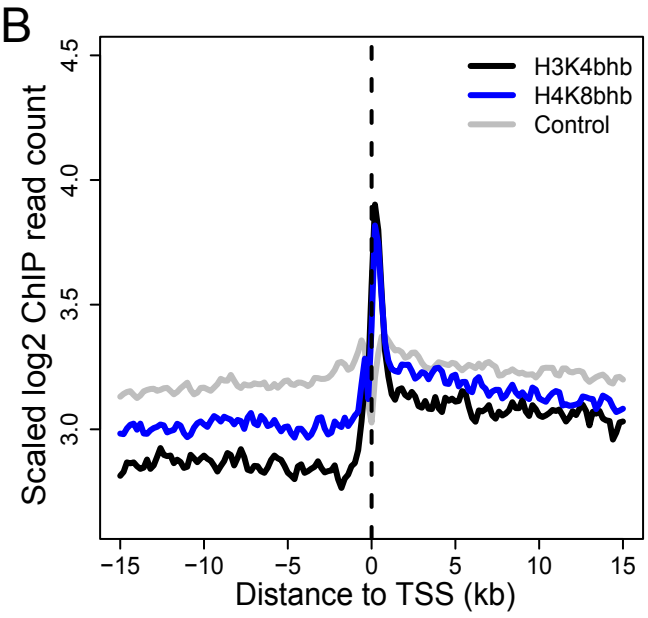

C

Correlation with RNAP II.Ser5P

	H3K9bhb	H3K9ac	H3K4me3	H3K27me3	H3K9me3
Coef. Est.	0.41	0.56	0.54	-0.29	-0.21
p-value	< 0.0001	< 0.0001	< 0.0001	< 0.0001	< 0.0001

Figure S4. Genome-Wide Localization of Histone Kbhb Marks, Related to Figure 5.

(A-B) Enrichment of histone Kbhb marks in promoter regions. ChIP profiles of H3K9bhb, H3K9ac, H3K4me3 and input control are shown in A); ChIP profiles of H3K4bhb, H4K8bhb and input control are shown in B). ChIP profiles represent ChIP read counts averaged using non-overlapping 200 base pair windows across all the genes, following the normalization across modifications so that baselines of ChIP profiles approximately match across different modifications.

(C) Correlation between RNAP II (Ser5p) and each of H3K9bhb, H3K9ac, H3K4me3, H3K27me3, and H3K9me3. See Supplemental Experimental Procedures for the statistics method.

Figure S5

A

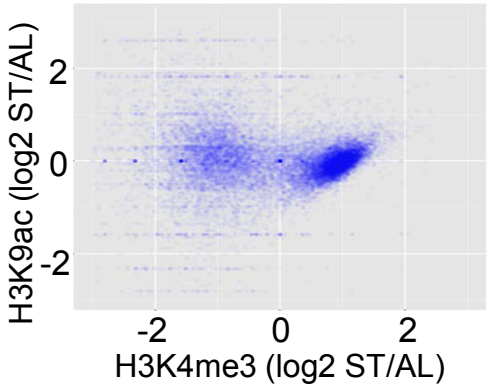

B

KEGG Pathway	NES	FDR
PATHWAYS_IN_CANCER	5.00	<0.001
HUNTINGTONS_DISEASE	4.36	<0.001
PARKINSONS_DISEASE	3.95	<0.001
ALZHEIMERS_DISEASE	3.94	<0.001
PROSTATE_CANCER	3.57	<0.001
CHRONIC_MYELOID_LEUKEMIA	3.49	<0.001
ACUTE_MYELOID_LEUKEMIA	3.49	<0.001
GLIOMA	3.25	<0.001
BASAL_CELL_CARCINOMA	3.19	<0.001
COLORECTAL_CANCER	3.15	<0.001
VIBRIO_CHOLERAE_INFECTION	2.89	<0.001
EPITHELIAL_CELL_SIGNALING_IN_HELICOBACTER_PYLORI_INFECTION	2.84	<0.001
PANCREATIC_CANCER	2.63	<0.001
ENDOMETRIAL_CANCER	2.60	<0.001
NON_SMALL_CELL_LUNG_CANCER	2.60	<0.001
THYROID_CANCER	2.50	<0.001
SMALL_CELL_LUNG_CANCER	2.30	0.001
TYPE_II_DIABETES_MELLITUS	2.27	0.001
PATHOGENIC_ESCHERICHIA_COLI_INFECTION	2.26	0.001

C

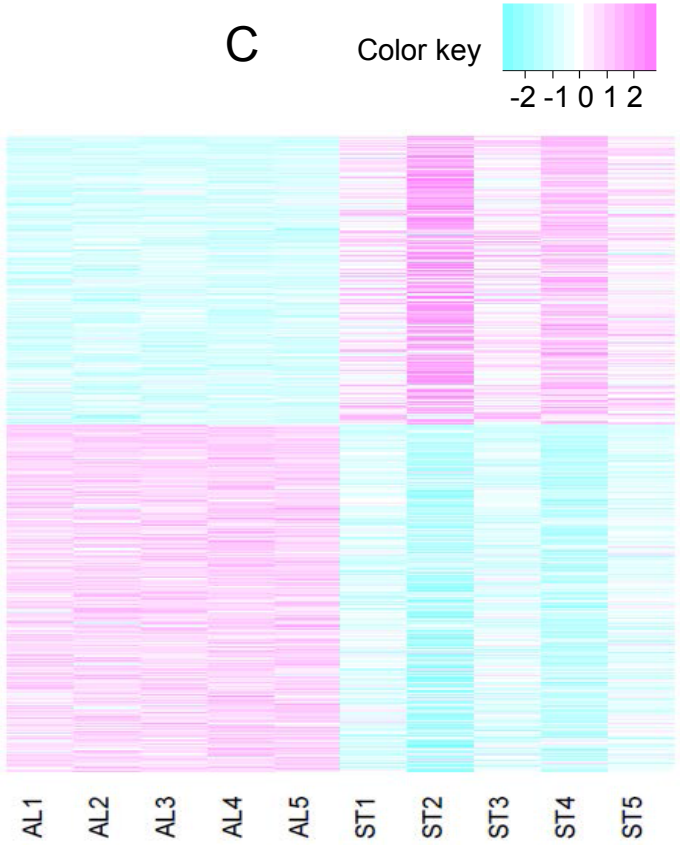

D Up-regulated genes Log2 (fold change) ≥0.5

KEGG_Pathway	NES	FDR
* RIBOSOME	6.06	<0.001
* OXIDATIVE_PHOSPHORYLATION	5.02	<0.001
SPLICEOSOME	4.83	<0.001
PROTEASOME	3.45	<0.001
RNA_DEGRADATION	2.30	0.007
* CIRCADIAN_RHYTHM_MAMMAL	2.16	0.012
* CYSTEINE_AND_METHIONINE_METABOLISM	2.12	0.015
UBIQUITIN_MEDIATED_PROTEOLYSIS	2.10	0.015
BASAL_TRANSCRIPTION_FACTORS	1.97	0.029
TGF_BETA_SIGNALING_PATHWAY	1.87	0.044
* ALANINE_ASPARTATE_AND_GLUTAMATE_METABOLISM	1.72	0.090
ADIPOCYTOKINE_SIGNALING_PATHWAY	1.72	0.083
* SELENOAMINO_ACID_METABOLISM	1.68	0.093
CARDIAC_MUSCLE_CONTRACTION	1.65	0.103
GLYCOSYLPHOSPHATIDYLINOSITOL_GPI_ANCHOR_BIOSYNTHESIS	1.59	0.123
CITRATE_CYCLE_TCA_CYCLE	1.53	0.150
AMINOACYL_TRNA_BIOSYNTHESIS	1.50	0.166
* PPAR_SIGNALING_PATHWAY	1.40	0.236
TRYPTOPHAN_METABOLISM	1.38	0.240

E Down-regulated genes Log2 (fold change) ≥0.5

KEGG_Pathway	NES	FDR
CHEMOKINE_SIGNALING_PATHWAY	4.71	<0.001
FOCAL_ADHESION	3.94	<0.001
AXON_GUIDANCE	3.55	<0.001
FC_GAMMA_R_MEDIATED_PHAGOCYTOSIS	3.52	<0.001
REGULATION_OF_ACTIN_CYTOSKELETON	3.50	<0.001
CELL_ADHESION_MOLECULES_CAMS	3.47	<0.001
CYTOKINE_CYTOKINE_RECEPTOR_INTERACTION	3.44	<0.001
VASCULAR_SMOOTH_MUSCLE_CONTRACTION	3.36	<0.001
NEUROACTIVE_LIGAND_RECEPTOR_INTERACTION	3.35	<0.001
DNA_REPLICATION	3.11	<0.001
CALCIUM_SIGNALING_PATHWAY	3.07	<0.001
FC_EPSILON_RI_SIGNALING_PATHWAY	2.96	<0.001
COMPLEMENT_AND_COAGULATION_CASCADES	2.87	<0.001
STEROID_BIOSYNTHESIS	2.81	<0.001
T_CELL_RECEPTOR_SIGNALING_PATHWAY	2.77	<0.001
OOCYTE_MEIOSIS	2.77	<0.001
LEUKOCYTE_TRANSENDOTHELIAL_MIGRATION	2.71	<0.001
INSULIN_SIGNALING_PATHWAY	2.63	<0.001

Figure S5. Starvation-Induced H3K9bhb is Associated with Active Gene Expression, Related to Figure 6.

(A) Correlation of changed ChIP-seq signals for H3K4me3 with those for H3K9ac upon starvation. Library sizes of ChIP-seq data were normalized between ST and AL conditions, for both modifications. Coef. Est. (overall) = -0.05, p-value (overall) = 0.2764; Coef. Est. (for H3K4me3 $\log_2$ ST/AL > 0) = 0.34, p-value (for H3K4me3 $\log_2$ ST/AL > 0) < 0.0001. See Supplemental Experimental Procedures for the statistics method.

(B) KEGG pathway analysis of H3K9bhb enriched disease related pathways using Gene Set Enrichment Analysis (GSEA). The top 20 pathways were listed, in the order of normalized enriched score (NES).

(C) Heat map of differentially expressed genes in response to starvation in RNA-seq data. “AL” indicates fed condition; “ST” indicates starved condition. Library sizes were normalized across samples, and the read counts per million (cpm) were log10 transformed and then centered and scaled in the row direction. Genes were ordered by $\log_2$ fold change of gene expression.

(D) KEGG pathway analysis of up-regulated genes in RNA-seq data by GSEA. 1742 up-regulated genes with Log_2 (fold change) ≥ 0.5 were subjected to KEGG pathway analysis. Top 20 pathways were shown in the table. Pathways with asterisk marks in front indicate that they are also presented in top H3K9bhb enriched pathways in ChIP-seq analysis (Figure 6D).

(E) KEGG pathway analysis of down-regulated genes in RNA-seq data by GSEA. 2104 down-regulated genes with Log2 (fold change) ≥ 0.5 were subjected to KEGG pathway analysis. Top 20 pathways were shown in the table.

Figure S6

A Common up-regulated non-disease pathway between H3K9bhb ChIP-seq and RNA-seq (top20)

KEGG_Pathway	NES	FDR
* RIBOSOME	6.79	<0.001
* OXIDATIVE_PHOSPHORYLATION	4.68	<0.001
SPLICEOSOME	4.46	<0.001
UBIQUITIN_MEDIATED_PROTEOLYSIS	3.30	<0.001
PROTEASOME	2.94	<0.001
WNT_SIGNALING_PATHWAY	2.83	<0.001
RNA_DEGRADATION	2.80	<0.001
* CIRCADIAN_RHYTHM_MAMMAL	2.77	<0.001
* CYSTEINE_AND_METHIONINE_METABOLISM	2.66	<0.001
ENDOCYTOSIS	2.63	<0.001
TGF_BETA_SIGNALING_PATHWAY	2.61	<0.001
INSULIN_SIGNALING_PATHWAY	2.40	0.003
* SELENOAMINO_ACID_METABOLISM	2.39	0.003
VALINE_LEUCINE_AND_ISOLEUCINE_DEGRADATION	2.29	0.006
RNA_POLYMERASE	2.27	0.006
BASAL_TRANSCRIPTION_FACTORS	2.23	0.009
VASOPRESSIN_REGULATED_WATER_REABSORPTION	2.21	0.009
* ALANINE_ASPARTATE_AND_GLUTAMATE_METABOLISM	2.17	0.011
AMINOACYL_TRNA_BIOSYNTHESIS	2.12	0.015
* PEROXISOME	2.12	0.015

B Common up-regulated disease related pathway between H3K9bhb ChIP-seq and RNA-seq (top20)

KEGG_Pathway	NES	FDR
HUNTINGTONS_DISEASE	4.82	<0.001
PARKINSONS_DISEASE	4.34	<0.001
ALZHEIMERS_DISEASE	3.65	<0.001
PATHWAYS_IN_CANCER	3.29	<0.001
PROSTATE_CANCER	2.34	0.003
EPITHELIAL_CELL_SIGNALING_IN_HELICOBACTER_PYLORI_INFECTION	2.26	0.005
BASAL_CELL_CARCINOMA	2.25	0.004
MELANOGENESIS	2.21	0.005
VIBRIO_CHOLERAE_INFECTION	2.12	0.008
ENDOMETRIAL_CANCER	1.97	0.016
CHRONIC_MYELOID_LEUKEMIA	1.89	0.023
COLORECTAL_CANCER	1.85	0.027
ACUTE_MYELOID_LEUKEMIA	1.85	0.025
BLADDER_CANCER	1.68	0.050
THYROID_CANCER	1.67	0.049
GLIOMA	1.62	0.059
PANCREATIC_CANCER	1.57	0.072
RENAL_CELL_CARCINOMA	1.52	0.086
SMALL_CELL_LUNG_CANCER	1.49	0.098
PATHOGENIC_ESCHERICHIA_COLI_INFECTION	1.36	0.162

C Common down-regulated non-disease pathway between H3K9bhb ChIP-seq and RNA-seq

KEGG_Pathway	NES	FDR
NEUROACTIVE_LIGAND_RECEPTOR_INTERACTION	3.08	<0.001
TERPENOID_BACKBONE_BIOSYNTHESIS	2.23	0.027
HEMATOPOIETIC_CELL_LINEAGE	2.04	0.059
CYTOKINE_CYTOKINE_RECEPTOR_INTERACTION	2.01	0.054
DNA_REPLICATION	1.84	0.109
CELL_ADHESION_MOLECULES_CAMS	1.74	0.164
NON_HOMOLOGOUS_END_JOINING	1.71	0.160
STEROID_BIOSYNTHESIS	1.69	0.153

D Common down-regulated disease-related pathway between H3K9bhb ChIP-seq and RNA-seq

KEGG_Pathway	NES	FDR
SYSTEMIC_LUPUS_ERYTHEMATOSUS	2.86	<0.001
PRIMARY_IMMUNODEFICIENCY	2.03	0.029
GRAFT_VERSUS_HOST_DISEASE	2.01	0.023
PRION_DISEASES	1.66	0.111
TYPE_I_DIABETES_MELLITUS	1.59	0.130
AUTOIMMUNE_THYROID_DISEASE	1.44	0.212
VIRAL_MYOCARDITIS	1.37	0.249

Figure S6. Common pathways in RNA-seq and ChIP-seq data, Related to Figure 6.

(A) Common up-regulated gene pathways in both H3K9bhb ChIP-seq data and RNA-seq data analyzed by GSEA, non-disease pathways. Top 20 pathways were shown in the table.

(B) Common up-regulated gene pathways in both H3K9bhb ChIP-seq data and RNA-seq data analyzed by GSEA, disease related pathways. Top 20 pathways were shown in the table.

(C) Common down-regulated gene pathways in both H3K9bhb ChIP-seq data and RNA-seq data analyzed by GSEA, non-disease pathways. Top pathways (FDR ≤ 0.25) were shown in the table.

(D) Common down-regulated gene pathways in both H3K9bhb ChIP-seq data and RNA-seq data analyzed by GSEA, disease related pathways. Top pathways (FDR ≤ 0.25) were shown in the table.

Figure S7

A

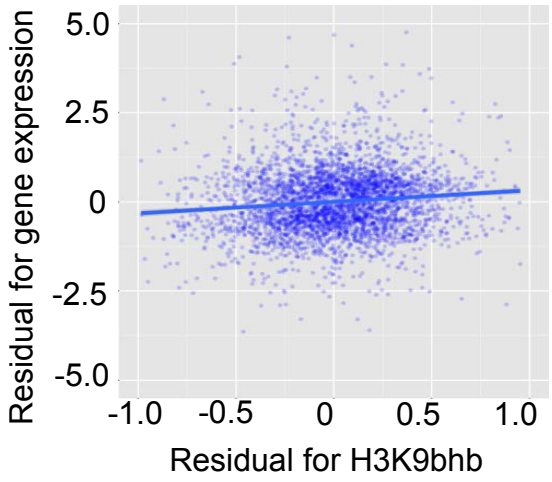

B

H3K9bhb exclusive pathway (175 genes)

KEGG Pathway	P-Value
Spliceosome	1.90E-03
Selenoamino acid metabolism	1.20E-02
PPAR signaling pathway	2.00E-02
Fatty acid metabolism	4.20E-02
Proteasome	4.60E-02

C

H3K9ac exclusive pathway (168 genes)

KEGG Pathway	P-Value
Retinol metabolism	2.60E-05
Purine metabolism	2.50E-03
Nucleotide excision repair	6.40E-03
Linoleic acid metabolism	7.70E-03
Metabolism of xenobiotics by cytochrome P450	2.00E-02
Drug metabolism	2.90E-02
Steroid hormone biosynthesis RT 3	6.00E-02
Drug metabolism	6.70E-02
Chemokine signaling pathway	7.70E-02

D

H3K4me3 exclusive pathway (145 genes)

KEGG Pathway	P-Value
Proteasome	1.60E-03
MAPK signaling pathway	4.30E-02

Figure S7. H3K9bhb Distinguishes a Set of Up-Regulated Genes from Others that Bear H3K9ac and H3K4me3 Marks, Related to Figure 6.

(A) Net association between H3K9bhb and gene expression, after excluding effects of H3K9ac and H3K4me3. X-axis and Y-axis indicate the H3K9bhb and gene expression values that are not explained by H3K4me3 and H3K9ac (i.e., the residuals of linear regression models of H3K9bhb and gene expression, respectively, on H3K9ac and H3K4me3). The line means the linear regression fit of the residuals for gene expression on the residuals for H3K9bhb. Coef. Est. = 0.14, p-value < 0.0001. See Supplemental Experimental Procedures for the statistics method.

(B-D) DAVID KEGG pathway analysis for genes marked exclusively by the increase of H3K9bhb (B), H3K9ac (C), and H3K4me3 (D) shown in Figure 6J, respectively. See also Figure 6J.

Table S1. Quantification of Kac on Histones from Control and Starved Mice Livers

Modification	Protein name	Modification site	Score	Modified sequence	Normalized ratios (fasted/fed)
Kac	Histone H1.2	H1 K74	100.45	_(pr)ALAAAGYDVEK(ac)NNSR_	2.75
	Histone H2A.Z	H2A K4, K7	89.548	_(pr)AGGK(ac)AGK(ac)DSGK(pr)_	0.99
	Histone H2A.J	H2A K5, K9	80.229	_(pr)GK(ac)QGGK(ac)VR_	1.38
	Histone H2B type 1-M	H2B K108	226.65	_(pr)LLLPGELAK(ac)HAVSEGTK(pr)_	2.27
	Histone H2B type 1-M	H2B K120	97.965	_(pr)AVTK(ac)YTSSK_	2.78
	Histone H3.1	H3 K9, K14	55.064	_(pr)K(ac)STGGK(ac)APR_	1.79
	Histone H3.1	H3 K18, K23	94.692	_(pr)K(ac)QLATK(ac)AAR_	1.47
	Histone H3.1	H3 K23	96.331	_(pr)QLATK(ac)AAR_	1.06
	Histone H3.1	H3 K56	95.401	_(pr)YQK(ac)STELLIR_	1.62
	Histone H4	H4 K5, K8, K12	65.563	_(pr)GK(ac)GGK(ac)GLGK(ac)GGAK(pr)_	1.25
	Histone H4	H4 K8, K12, K16	129.89	_(pr)GGK(ac)GLGK(ac)GGAK(ac)R_	1.52
	Histone H4	H4 K12, K16	113.71	_(pr)GLGK(ac)GGAK(ac)R_	1.40
	Histone H4	H4 K59	64.55	_(pr)GVLK(ac)VFLENVIR_	1.52

Note:

Pr- propionylation (lysine or peptide N-terminal)

Pm- propmethyl (lysine)

Ac- acetylation (lysine)

Bhb- β-hydroxybutyrylation (lysine)

Table S1. Quantification of Kac on Histones from Control and Starved Mice Livers, Related to Table 1. The liver histone samples from either control (fed) mice or fasted mice (fasted for 48h) were labeled with 12C6-propionic anhydride or 13C6-propionic anhydride respectively. Two chemical propionylation methods were used (before tryptic digestion and after tryptic digestion). The peptides with N-terminal propionylation were derived from propionylation after tryptic digestion. The peptides without N-terminal propionylation were derived from propionylation before tryptic digestion. The resulting tryptic digested peptides were enriched by pan anti-Kbhb antibody, followed by LC/MS/MS analysis. The normalized peptide ratios were based on normalization with protein ratios.

Table S2. A List of Genes Up-Regulated during Starvation in RNA-Seq Data, Related to Figure 6. In this table, “logFC” and “logCPM” are the log2 fold change upon starvation and the log 2 counts-per-million averaged over all the libraries, respectively. “PValue” is the p-value from the hypothesis testing for differential expression and “FDR” is the p-value adjusted for multiple testing using the Benjamini-Hochberg method. Genes are sorted by the FDR values

Table S3. A List of Genes Down-Regulated during Starvation in RNA-seq Data, Related to Figure 6. In this table, “logFC” and “logCPM” are the log2 fold change upon starvation and the log 2 counts-per-million averaged over all the libraries, respectively. “PValue” is the p-value from the hypothesis testing for differential expression and “FDR” is the p-value adjusted for multiple testing using the Benjamini-Hochberg method. Genes are sorted by the FDR values.

Table S4. **A List of Genes in Top10 H3K9bhb Enriched KEGG Pathways during Starvation in ChIP-seq Data, Related to Figure 6.** Each tab corresponds to each of the 10 KEGG pathways presented in Figure 6D, and each tab provides a table of genes in the pathway and their percentiles in H3K9bhb, H3K9ac, and H3K4me3 ChIP-seq data in the sense of increase upon starvation. For example, in the circadian rhythm pathway, the increase of H3K9bhb in promoter regions of PER1 and PER2 correspond to top 1% and top 10%.

Data S1. Annotated MS/MS spectra of histone Kbhb-containing peptides from R-β-hydroxybutyrate-[2, 4-$^{13}C_2$]-treated HEK293 cells, Related to Figure 4. The fragment ions were labeled by Mascot.

Data S2. Annotated MS/MS spectra of histone Kbhb-containing peptides from sodium-R-β-hydroxybutyrate-treated HEK293 cells, Related to Figure 4. The fragment ions were labeled by Mascot.

Data S3. Annotated MS/MS spectra of histone Kbhb-containing peptides from liver cells, isolated from either fasted or STZ-induced diabetic mice, Related to Figure 4. The fragment ions were labeled by Mascot.

SUPPLEMENTAL EXPERIMENTAL PROCEDURES

Reagents

Antibodies: The pan anti-Kbhb, sequence-specific anti-H3K9bhb, -H3K4bhb, -H3K18bhb and -H4K8bhb antibodies were from PTM Biolabs, Inc. (Chicago, IL); Anti-histone H3 (ab12079), -H3K9ac (ab4441), -H3K4me3 (ab8580) and –Pol II (Ser5p) (ab5131) antibodies were from Abcam (Cambridge, MA). Peptides were synthesized using protected amino acid residues. Synthesis of Fmoc-protected modified lysine residues is described in detail below. Modified sequencing-grade trypsin was purchased from Promega (Madison, WI). C_{18} ZipTips were bought from Millipore Corporation (Bedford, MA). Other chemicals were obtained from the following suppliers. Sigma-Aldrich (St. Louis, MO): formic acid (>98%), NH_4HCO_3 (>99%), trichloroacetic acid (6.1 N), iodoacetamide, dithiothreitol, bovine serum albumin, sodium butyrate, nicotinamide, trichostatin A, Fmoc-Lys-OH (98%), Sodium (R/S)-3-Hydroxybutyrate-2,4-$^{13}C_2$ (99%), (R/S)-3-hydroxybutyrate, (R)-3-hydroxybutyrate, (S)-3-hydroxybutyrate, 2-hydroxyisobutyric acid (98%), N-hydroxysuccinimide (98%), H_3PO_4 (99%), BF3•OEt2, isobutylene (99%), LiOH (>98%), 4-butyrolactone (>99%), trityl chloride (98%), anhydrous pyridine (99.8%), ethyl (R)-3-hydroxybutyrate (98%), ethyl (S)-3-hydroxybutyrate (99%), N,N'-dicyclohexylcarbodiimide (DCC) (99%), anhydrous dioxane (99.8%), methyl (S)-3-hydroxy-2-methylpropionate (99%), methyl (R)-3-hydroxy-2-methylpropionate (99%), trifluoroacetic acid (99%), and ethyl 2-hydroxybutyrate (>95% GC). Fisher (Pittsburgh, PA): $NaHCO_3$ (ACS grade), NaOH (ACS grade), CH_3CN (HPLC grade), CH_2Cl_2 (HPLC grade), HCl solution (37.3%), MeOH (ACS grade), acetone (ACS grade), EtOAc (ACS grade), anhydrous Et2O (ACS grade), DMEM medium (high glucose), anhydrous Na_2SO_4 (ACS grade), anhydrous $MgSO_4$ (ACS grade), hexane (ACS grade), Et3N (>99%), and hydrogen peroxide.

Animal experiments

For the starvation experiment, two groups of 16 weeks old adult C57BL/6 mice (control group: n =20, 10 males and 10 females; experimental group: n=30, 15 males and 15 females) were either fed with standard chow diet containing 19% protein, or fasted (with free access to water) for 48 hours (9:00 am to 9:00 am) as detailed in the text.

C57BKS/J db/db mice were licensed from the Jackson Laboratory and bred in house. All mice were housed in a temperature-controlled room (22 ± 2 °C), with a light/dark cycle of 12h/12h. At the age of 12 weeks, C57BKS/J db/db littermates (C57BLKS/J lean mice) were recruited to the experiment and randomly assigned. For the ketoacidosis experiment, db-littermate mice (n =6 for each group, 3 males and 3 females) were either given single-dose intraperitoneal injections of streptozotocin (STZ, 200 mg/kg body weight), or the sodium citrate buffer vehicle. After 48 hrs, blood samples were taken from a tail vein for determination of blood glucose and β-hydroxybutyrate concentrations using a gluco-ketone meter (Lifescan, Burnaby, BC, Canada). The mice were decapitated and liver tissue was collected for histone extraction and lysate preparation.

Metabolite extraction:

Total metabolites from cell line and mouse liver were extracted according to protocol published (Liu et al., 2015) with modification. Briefly, when cell line was used, cells was washed quickly with ice cold PBS and placed on dry ice. One milliliter of extraction buffer (80% methanol in water) was added to the plate and transferred to -80 degree. Fifteen minutes later, cells were scraped in extraction buffer and centrifuged at 20,000g for 15 min in the cold room. Supernatant was collected carefully and dried by SpeedVac. For frozen mouse liver tissue, the tissue was first homogenized in liquid nitrogen. Twenty mg of tissue powder was weighed and placed in a 2ml dounce homogenizer on ice. One milliliter of extraction buffer (80% methanol in water) was added and the tissue was homogenized for 30 strokes. The extraction was transferred and centrifuged at 20,000g for 15 min in the cold room. Supernatant was collected carefully and dried by SpeedVac.

Metabolite detection and analysis:

Crude metabolites extracts were dissolved into 10 µl of sample buffer (water with 25 mM ammonium acetate, pH = 6.8). The mixture was diluted to 50-fold and 2500-fold water with sample buffer for cell and liver samples, respectively. Samples were centrifuged at 20,000 g at 4 °C for 5 min, and 5 µl of the supernatant was loaded onto a home-made capillary column (10 cm length with 75 um inner diameter) packed with Jupiter C12 resin (4 µm particle size, 90 Å pore size, Phenomenex) connected to a NanoLC-1D plus HPLC system (Eksigent Technologies, Dublin, CA) for Acyl-CoA analysis. The loaded samples were eluted with a fixed gradient of 90% HPLC buffer B (95% ACN in water with 5 mM ammonium acetate, pH = 6.8) in buffer A (water with 5 mM ammonium acetate, pH = 6.8) at a flow rate of 900 nL/min over 20 min. The eluted CoAs were electrosprayed into a LTQ-Orbitrap Velos mass spectrometer (ThermoFisher Scientific, Waltham, MA) operating in a focused ion mode. A full MS scans were acquired in the Orbitrap mass analyzer over the range m/z 700-1000 with a mass resolution of 15000 at m/z 400. The MS/MS of focused ions (Acetyl-CoA, 810.13 → 303.14 m/z; Bhb-CoA, 854.16 → 347.16; isotopic Bhb-CoA: 858.17 → 351.18) were acquired over the range m/z 50-1000 with a mass resolution of 7500 at m/z 400 using higher energy collisionally activated dissociation (HCD) in the Orbitrap mass analyzer at 35% normalized collision energy. Data was acquired and analyzed using Xcalibur 2.1.0 software (Thermo Fisher Scientific).

Extraction of histones

Extraction of core histones from HEK293 cells and mouse liver were carried out according to previously published papers (Shechter et al., 2007). Liver samples were homogenized using a glass Dounce homogenizer (20 strokes) in ice-cold lysis buffer. The homogenate was passed through two layers of cheese cloth and then centrifuged at 1,000 g at 4 °C for 5 min. The pellet was briefly washed with lysis buffer and extracted with 0.4 N H_2SO_4 at 4 °C overnight. HEK293 cells were lysed in lysis buffer on ice for 10 min with gentle stirring. The lysate was removed and the pellet was washed once with the lysis buffer and then extracted with 0.4 N H_2SO_4 at 4 °C overnight. The suspension was centrifuged at 20,000 x g for 10 min at 4 °C. The histone-

containing supernatants were precipitated with 20% trichloroacetic acid. The precipitated histone pellets were washed twice with cold acetone and dried. The histone samples were then digested with sequencing grade trypsin as described earlier.

Chemical Propionylation

To quantify histone lysine acetylation or β-hydroxybutyrylation levels from mouse under fed and fasting conditions, we did in *vitro* propionylation either before or after tryptic digestion, labeling with ^{12}C or ^{13}C propionic anhydride respectively. The procedure is similar to the reported methods (Dai et al., 2014; Garcia et al., 2007), but with minor modifications. Briefly, 250ug each of histones (for propionylation before tryptic digestion) or histone peptides (for propionylation after tryptic digestion) from two conditions (fed or fasted) were prepared in 300 µl of 0.1 M NH_4HCO_3 buffer, pH 8.0. We added 3uL of propionic anhydride (7.8M) (^{12}C -propionic anhydride for fed sample, ^{13}C-propionic anhydride for fasted sample) to the sample and adjusted pH to 7~8 by dropping NaOH little by little. After incubating for 1hr in RT, we did a second round of propionylation to enhance labeling efficiency. After the reaction, 3 uL of Ethanolamine was added to incubate for 60 min in RT using vortex shaker.

HPLC-mass spectrometry analysis

Tryptic peptides were dissolved in HPLC buffer A (0.1% formic acid in water) and loaded onto a self-packed capillary column (10 cm in length, 75 µm ID) packed with Jupiter C12 resin (Phenomenex, 90 Å, 4 µm in size) by Eksigent 1D-plus nano-flow HPLC. Peptides were eluted with a linear gradient of 5%-30% B in 2 hrs with a constant flow rate of 200 nL/min. Peptide ions were directly electro sprayed into a LTQ Velos Orbitrap mass spectrometer and analyzed by either fragmenting the 20 most intense ions in a data-dependent mode, or fragmenting specified precursor ions for targeted analysis by collision-induced dissociation.

Peptide identifications and quantifications

MS/MS data were analyzed by Mascot (version 2.1, Matrix Science Ltd, London, UK) against an IPI human (v3.70) or IPI mouse (v3.74) database for protein and peptide identification. Lys acetylation, β-hydroxybutyrylation, methionine oxidation, and protein N-terminal acetylation were specified as variable modifications. Mass tolerance was set to 20 ppm for precursor ions and 0.5 Da for fragment ions. To reduce the number of low quality PTM identifications, we further removed all peptides with Mascot peptide score below 20, and all peptides with C-terminal Lys modifications (unless the modified peptides are protein C-terminal peptides). All the detected Kbhb-modified peptides were manually inspected to ensure high quality of peptide identification. Peptides quantification was performed with Maxquant (version 1.3.0.5) against an IPI human (v3.70) or IPI mouse (v3.74) database. Variable modifications were set as same as those for Mascot. Results were filtered by a 1% false discovery rate at protein, peptide and site levels. We also removed the peptides with Maxquant score below 40 or site localization probability below 0.75, and the peptides with C-terminal Lys modifications (unless the modified peptides are protein C-terminal peptides).

Primer sequences for ChIP-qPCR and RT-qPCR

ChIP experiments for histone marks were carried out according to the instructions from the ChIP-IT® High Sensitivity kit (Active Motif, Carlsbad, CA). ChIP DNA and input DNA were analyzed by qPCR using SYBR® Select Master Mix (Life Technologies, Thermo Fisher Scientific Inc., Waltham, MA) and StepOnePlus Real-Time PCR system (Applied Biosystems, Thermo Fisher Scientific Inc., Waltham, MA). The sequences for ChIP-qPCR primers are:

Hnf4a-up: forward- AGGCTTGGGAGGAGAATCAT; reverse- CAGGACAGGCACAGACAAGA;

Hnf4a-promoter: forward- GTACTGTGGCCAGAGGCATT; reverse- GAGGGTCTGGGGAATTTTTC;

Hnf4a-intron: forward- TATGTGTCTGTGGGGTGGTG; reverse- GCCATCTCTCTCTCCAGTGC;

Hnf4a-down: forward- TCTAGGGGGATGTTGGAGCT; *Hnf4a*-down: reverse- AGGCAAATACCACCCTGCTC;

Per1: forward- CACTCTAGGGTCCCTGGACA; reverse- GCTCTCAGGGGTCATATCGC;

Cry1: forward- GAGTCCCTTTCGGAACCAGT; reverse- CTTCCCTCCCTTGAAGCTCT;

Hnf4a: forward- GTACTGTGGCCAGAGGCATT; reverse- GAGGGTCTGGGGAATTTTTC;

Irs2: forward- GAGGCACTACCGCTGGAC; reverse- CCTCATCCACTGCATCACC;

Ppargc1b: forward- GAGAGCTGGAAGACGCAATC; reverse- TGCTGGCTAGGGGAATAGG;

Cpt1a: forward- AAGCAGAGGACTGTGGTGTG; reverse- TAGCCCAGGACTCTGAATGC;

Socs3: forward- GCAGCCGTGAAGTCTACAAA; reverse- CCAGGTCCTTTGCCTGATT;

Serpina: forward- GGCTGGCTTGAAGACGAAGA; reverse- GGAGCTTGTCTTCTTGGCCT.

Total RNAs were extracted from mouse livers using the RNeasy Mini Kit (QIAGEN INC, Valencia, CA). cDNA was prepared using RevertAid First Strand cDNA Synthesis kit (Thermo Fisher Scientific Inc., Waltham, MA) following manufacture's protocol and analyzed by qPCR using SYBR® Select Master Mix (Life Technologies, Thermo Fisher Scientific Inc., Waltham, MA) and StepOnePlus Real-Time PCR system (Applied Biosystems, Thermo Fisher Scientific Inc., Waltham, MA). The sequences for RT-qPCR primers are:

Per1: forward- CGTCCTACCTCCTTTATCCAGA; reverse- TGTTTGCATCAGTGTCATCAGC;

Cry1: forward- CTGGCGTGGAAGTCATCGT; reverse- CTGTCCGCCATTGAGTTCTATG;

Hnf4a: forward- ACCAAGAGGTCCATGGTGTTT; reverse- GTGCCGAGGGACGATGTAG;

Cpt1a: forward-CTCCGCCTGAGCCATGAAG; reverse- CACCAGTGATGATGCCATTCT;

Socs3: forward- CCCTTGCAGTTCTAAGTTCAACA; reverse- ACCTTTGACAAGCGGACTCTC;

Irs2: forward- CTGCGTCCTCTCCCAAAGTG; reverse- GGGGTCATGGGCATGTAGC;

Ppargc1b: forward- TCCTGTAAAAGCCCGGAGTAT; reverse- GCTCTGGTAGGGGCAGTGA;

Serpina5: forward- AGAAGAAGGCTAAAGAGTCCTCG; reverse- CTCATAGACACGCTCAAGGGG.

Actin: forward-ACCTTCTACAATGAGCTGCG; reverse-CTGGATGGCTACGTACATGG.

ChIP-seq and RNA-seq analyses

ChIP-seq analysis:

Chromatin Immunoprecipitation for histone marks were carried out according to the instructions from the ChIP-IT® High Sensitivity kit (Active Motif, Carlsbad, CA), except that chromatin was prepared by MNase digestion (Delaval et al., 2007). For each reaction, 100 mg of pooled control or starved mice liver tissue was used. 5 ug pan anti-Kbhb antibody or 3µg each of anti-H3K4bhb, -H3K9bhb, -H4K8bhb, -H3K9ac and -H3K4me3 antibodies were used per reaction. ChIP-seq libraries were prepared following the Ovation Ultralow DR Multiplex System protocols (NuGEN Technologies INC, San Carlos, CA), followed by a size selection (200-700bp) step by SPRIselect beads (Beckman Coulter, Brea, CA). The libraries were sequenced on Illumina HiSeq 2500 machine at the University of Chicago Genomics Core as per manufacturer's protocols.

ChIP-seq reads were mapped to the reference genome of Illumina iGenomes UCSC MM10 (http://support.illumina.com/sequencing/sequencing_software/igenome.ilmn) using Bowtie (Langmead et al., 2009) version 0.12.7, allowing up to two mismatches, and only the uniquely mapped reads were retained. Cross-correlation analysis (Landt et al., 2012) and signal enrichment analysis were implemented for the quality control purpose and no significant quality problems were detected. Peaks were called using MOSAiCS (Chung et al., 2014; Kuan et al., 2011) version 2.0.0 with FDR = 1e-10. In order to avoid peak caller bias issue, we also called peaks using MACS (Zhang et al., 2008) and SPP (Kharchenko et al., 2008) and then, compared their results with the results from MOSAiCS. While both MACS and SPP still show consistent results, MOSAiCS outperformed them and provided the peak calling results that were most consistent with visual inspection. Finally, based on the observation that bhb modifications are highly enriched in the promoter regions, we used following measurements for the downstream analysis. 1) We summarized ChIP read counts in promoter region of each gene (+/-2kb around TSS). Let's denote ST_j and AL_j be the ChIP read counts in promoter region of j-th gene under the ST and AL conditions, respectively. 2) We normalize them between ST and AL conditions by defining $AL_j^{adj} = AL_j * \Sigma_k ST_k / \Sigma_k AL_k$, where $\Sigma_k ST_k$ and $\Sigma_k AL_k$ are summations of ST_j and AL_j over all the genes, respectively. When we calculated these summations, we excluded 10% genes with the largest ChIP read counts and 10% genes with the smallest ChIP read counts in each condition, to avoid effects of outliers (i.e., genes with extremely large and small ChIP counts). 3) We calculated the log2-transformed ratio of ChIP read counts between ST and AL, i.e, $\log_2 (ST_j / AL_j^{adj})$, and used it for the downstream analysis. KEGG Pathway analysis was implemented using GSEA (Gene Set Enrichment Analysis) (Mootha et al., 2003; Subramanian et al., 2005). The list of KEGG pathways (CP: KEGG) from MSigDB (http://www.broadinstitute.org/gsea/msigdb/genesets.jsp?collection=CP:KEGG) was used for the enrichment analysis. To better focus on normal physiology process, disease-related pathways in the database were extracted for a separate analysis, including: KEGG_ACUTE_MYELOID_LEUKEMIA, KEGG_ALLOGRAFT_REJECTION, KEGG_ALZHEIMERS_DISEASE, KEGG_AMYOTROPHIC_LATERAL_SCLEROSIS_ALS, KEGG_ARRHYTHMOGENIC_RIGHT_VENTRICULAR_CARDIOMYOPATHY_ARVC, KEGG_ASTHMA, KEGG_AUTOIMMUNE_THYROID_DISEASE, KEGG_BASAL_CELL_CARCINOMA, KEGG_BLADDER_CANCER, KEGG_CHRONIC_MYELOID_LEUKEMIA, KEGG_COLORECTAL_CANCER, KEGG_DILATED_CARDIOMYOPATHY, KEGG_ENDOMETRIAL_CANCER, KEGG_EPITHELIAL_CELL_SIGNALING_IN_H, ELICOBACTER_PYLORI_INFECTION, KEGG_GLIOMA, KEGG_GRAFT_VERSUS_HOST_DISEASE,

KEGG_HUNTINGTONS_DISEASE, KEGG_HYPERTROPHIC_CARDIOMYOPATHY_HCM, KEGG_LEISHMANIA_INFECTION, KEGG_MATURITY_ONSET_DIABETES_OF_THE_YOUNG, KEGG_MELANOGENESIS, KEGG_MELANOMA, KEGG_NON_SMALL_CELL_LUNG_CANCER, KEGG_PANCREATIC_CANCER, KEGG_PARKINSONS_DISEASE, KEGG_PATHOGENIC_ESCHERICHIA_COLI_INFECTION, KEGG_PATHWAYS_IN_CANCER, KEGG_PRIMARY_IMMUNODEFICIENCY, KEGG_PRION_DISEASES, KEGG_PROSTATE_CANCER, KEGG_RENAL_CELL_CARCINOMA, KEGG_SMALL_CELL_LUNG_CANCER, KEGG_SYSTEMIC_LUPUS_ERYTHEMATOSUS, KEGG_THYROID_CANCER, KEGG_TYPE_I_DIABETES_MELLITUS, KEGG_TYPE_II_DIABETES_MELLITUS, KEGG_VIBRIO_CHOLERAE_INFECTION, KEGG_VIRAL_MYOCARDITIS.

In some places (Figures S5I-S5K), pathway analysis was carried out using DAVID (Huang da et al., 2009a, b).

RNA-seq analyses:

Total RNAs were extracted from frozen mouse liver tissue using the RNeasy Mini Kit (QIAGEN INC, Valencia, CA). The sequencing libraries were constructed according to manufacturer instructions using TruSeq Stranded Total Sample Preparation kit (Illumina, San Diego, CA). RNAseq reads were mapped to iGenome UCSC MM10 gene annotation using TopHat (Trapnell et al., 2009) version 2.0.0. Mapped reads were summarized for each gene using HTSeq (Anders et al., 2015) version 0.6.1. Differential expression analysis was implemented using edgeR (Robinson and Smyth, 2007, 2008) version 3.6.4 with FDR = 0.05 and at least 0.5 absolute $\log_2$ fold change, after retaining only the genes of which counts per million (cpm) is larger than one in at least five samples and normalizing the library sizes across samples using the TMM method of edgeR package. KEGG Pathway analysis was implemented using GSEA (Gene Set Enrichment Analysis), in the same way as in ChIP-seq KEGG Pathway analysis.

About correlation analysis :

In order to avoid potential inflation of statistical significance for correlation due to large number of genes used for hypothesis testing, we calculated all the p-values for correlation coefficient in the manuscript using the following subsampling approach. First, we subsampled 1,000 genes from the full set of genes and calculated the correlation coefficients using only these 1,000 genes. Note that 1,000 genes correspond to less than 5% of the total number of mouse genes. We iterated this analysis 10,000 times with different random seeds. Then, for the hypothesis testing of H0: correlation coefficient = 0, we calculated p-value =2 * min ([number of iterations that subsampled correlation coefficient < 0], [number of iterations that subsampled correlation coefficient > 0]) / [# iteration].

Chemical synthesis

Fmoc-Lys ((±)-2-(^{t}BuO) butyryl)-OH.

Step 1. Racemic ethyl 2-hydroxybutyrate (15.1 mmol, 1.78 g, 1.83 ml) was dissolved in 25 ml CH_2Cl_2. Then, 2 g of 99% H_3PO_4 and 312 µl $BF_3{\cdot}OEt_2$ was added in sequential order. The resulting mixture was cooled in an ice acetone bath and stirred. Then, 10 ml isobutylene

measured in a 50-ml cylinder (precooled in dry ice acetone bath) was poured into the flask. The flask was sealed, and the reaction was stirred under –78 °C for 1 h and allowed to return to room temperature. After 10 h, the isobutylene was discharged, and the solvent was evaporated to dryness. The residue was redissolved in 100 ml EtOAc. The solution was washed three times with saturated $NaHCO_3$ solution, followed by brine. The organic layer was separated and dried over anhydrous Na_2SO_4. The solvent was evaporated, and the residue was purified through flash column chromatography. The column was first eluted with 50 ml hexane/triethylamine (v/v = 50/1) and then with 200 ml hexane/CH_2Cl_2 (v/v = 7/1), followed by 200 ml hexane/EtOAc (v/v = 8/1). A yield of 1.31 g (50%) ethyl 2-(^{t}BuO) butyrate was obtained.

Step 2. Ethyl 2-(^{t}BuO) butyrate (1.31 g, 7 mmol) was dissolved in 20 ml MeOH/H_2O = 1:1 solution. Then, LiOH (25 mmol, 575 mg) was added. The mixture was stirred at room temperature for 1.5 h. 50 ml water was added. The solution was washed with Et_2O (30 ml × 2) to remove some impurities. Then, the aqueous layer was separated and acidified with 1 M HCl solution to pH 2.3. The aqueous solution was extracted three times with EtOAc. The organic layer was combined, washed with brine and dried over anhydrous Na_2SO_4. The solvent was filtered and evaporated to give the crude product 2-(^{t}BuO) butyric acid, which was used in the next step without further purification.

Step 3. N,N'-dicyclohexylcarbodiimide (DCC,6.5 mmol, 1.31 g) was added to a solution (80 ml) of 2-(^{t}BuO) butyric acid (1.04 g, 6.5 mmol) and N-hydroxy-succinimide (6.5 mmol, 748 mg) in CH_3CN. The reaction was stirred at room temperature for 4 h. The resulting suspension was filtered and concentrated under vacuum. The residue was redissolved in 100 ml CH_2Cl_2. Et_3N (13 mmol, 1.81 ml) and Fmoc-Lys-OH (6.5 mmol, 2.62 g) were sequentially added. The reaction mixture was stirred at room temperature for 8 h and then evaporated, and the residue was dissolved in 150 ml water. The solution was adjusted to pH 2.3. The organic layer was separated, and the aqueous layer was extracted 3 times with EtOAc. The combined organic layers were dried over anhydrous Na_2SO_4. The residue was purified through flash column chromatography (eluent: MeOH/CH_2Cl_2 = 1:40 to 1:20). A yield of 2.5 g (75%) Fmoc-Lys (2-(^{t}BuO) butyryl)-OH was obtained. ^{1}H NMR (500 MHz, $CDCl_3$): δ 9.73 (s, 1H), 7.73 (d, J = 7.5 Hz, 2H), 7.54–7.61 (m, 2H), 7.36 (t, J = 7.5 Hz, 2H), 7.28 (t, J = 7.5 Hz, 2H), 6.87–6.90 (m, 1H), 5.85 (dd, J = 27.5, 9.0 Hz, 1H), 4.28–4.44 (m, 3H), 4.15–4.19 (m, 1H), 3.91–3.94 (m, 1H), 3.19–3.36 (m, 2H), 1.38–1.92 (m, 8H), 1.17 (1.15) (s, 9H), 0.88 (q, J = 7.0 Hz, 3H); ^{13}C NMR (125 MHz, $CDCl_3$): δ 175.7, 174.6, 156.1, 143.87 (143.86, 143.70, 143.68), 141.2, 127.6, 127.0, 125.2 (125.1), 119.8, 75.3 (75.2), 73.6 (73.5), 67.0, 53.6, 47.1, 38.4 (38.4), 31.84 (31.2), 29.22 (29.16), 27.89 (27.87), 27.67 (27.66), 22.22 (22.18), 9.42 (9.36); IR (KBr): 3404, 3336, 3065, 2973, 2936, 2875, 1718, 1632, 1538, 1451, 1338, 1255, 1192, 1107, 1081, 1057, 1005, 760, 740 cm^{-1}; HRMS (m/z): $[M]^+$ calcd. for C29H39N2O6, 511.2808; found, 511.2787.

Synthesis of Fmoc-Lys ((±)-3-(^{t}BuO) butyryl)-OH and Fmoc-Lys ((±)-3-(^{t}BuO) isobutyryl)-OH are synthesized in a similar manner as Fmoc-Lys ((±)-2-(^{t}BuO) butyryl)-OH starting from different raw materials.

Fmoc-Lys((±)-3-(^{t}BuO) butyryl)-OH: ^{1}H NMR (500 MHz, $CDCl_3$): δ 9.23 (s, 1H), 7.73 (d, J = 7.5 Hz, 2H), 7.58 (t, J = 7.5 Hz, 2H), 7.36 (t, J = 7.5 Hz, 2H), 7.27 (t, J = 7.5 Hz, 2H), 6.87–6.89 (m, 1H), 5.85 (d, J = 8.0 Hz, 1H), 4.33–4.46 (m, 3H), 4.16–4.19 (m, 1H), 4.01–4.07 (m, 1H), 3.31–3.38 (m, 1H), 3.12–3.18 (m, 1H), 2.61 (ddd, J = 52.5, 14.5, 6.5 Hz, 2H), 1.78–1.95 (m, 2H), 1.38–1.57 (m, 4H), 1.15–1.16 (m, 12H); ^{13}C NMR (125 MHz, $CDCl_3$): δ 174.6, 172.4, 156.1, 143.9 (143.7), 141.2, 127.6, 126.99 (126.97), 125.12 (125.09), 119.9, 74.7, 66.9, 65.1, 53.6, 47.1, 45.2, 38.9, 31.9, 28.9, 28.2, 22.8, 22.3; IR (KBr): 3332, 3065, 2974, 2935, 2869, 1718, 1653, 1541, 1450, 1366, 1208, 1106, 1084, 1053, 989, 760, 740 cm^{-1}; HRMS (m/z): $[M]^+$ calcd. for C29H39N2O6, 511.2808; found, 511.2787.

Fmoc-Lys((±)-3-(^{t}BuO) isobutyryl)-OH: ^{1}H NMR (500 MHz, $CDCl_3$): δ 9.76 (s, 1H), 7.72 (d, J = 7.5 Hz, 2H), 7.58 (dd, J = 10.0, 8.0 Hz, 2H), 7.35 (t, J = 7.5 Hz, 2H), 7.26 (t, J = 7.5 Hz, 2H), 6.85 (t, J = 6.0 Hz, 1H), 5.91 (t, J = 8.0 Hz, 1H), 4.29–4.41 (m, 3H), 4.16–4.18 (m, 1H), 3.38–3.39 (m, 2H), 3.18–3.30 (m, 2H), 2.42–2.48 (m, 1H), 1.47–1.94 (m, 2H), 1.41–1.53 (m, 4H), 1.14 (s, 9H), 1.11 (d, J = 7.5 Hz, 3H); ^{13}C NMR (125 MHz, $CDCl_3$): δ 176.2 (176.1), 174.6, 156.2, 143.8 (143.7), 141.1, 127.5, 126.9, 125.09 (125.05), 119.8, 73.6, 66.9, 63.8 (63.7), 53.6, 47.0, 40.99 (40.97), 38.8, 31.7, 29.0, 27.265 (27.260), 22.2, 14p.0 (13.9); IR (KBr): 3334, 3066, 2974, 2927, 2872, 1726, 1657, 1541, 1450, 1364, 1335, 1235, 1028, 876, 760, 739 cm^{-1}; HRMS (m/z): $[M]^{+}$ calcd. for C29H39N2O6, 511.2808; found, 511.2791.

Fmoc-Lys (2-hydroxyisobutyryl)-OH.

DCC (32.6 mmol, 6.72 g) was added to a solution of 2-hydroxyisobutyric acid (32 mmol, 3.35 g) and N-hydroxysuccinimide (32.6 mmol, 3.75 mg) in 30 ml anhydrous CH3CN. The resulting mixture was stirred at room temperature for 3 h and then filtered. The filtration was evaporated to dryness. The residue was re-dissolved in 300 ml CH_2Cl_2, and Et_3N (64 mmol, 8.9 ml) and Fmoc-Lys-OH (32 mmol, 12.9 g) were added. The mixture was stirred at room temperature for 8 h. The solvent was evaporated, and the residue was redissolved in water. The pH of the solution was adjusted to 2.0. The aqueous solution was extracted three times with ethyl acetate. The organic phases were combined, washed with brine and dried over anhydrous Na_2SO_4. The solvent was reduced to dryness, and the residue was purified through flash column chromatography (eluent: $MeOH/CH_2Cl_2$ = 1:40 to 1:20). A yield of 8.7 g (60%) Fmoc-Lys (2-hydroxyisobutyryl)-OH was obtained. Fmoc–Lys(2–hydroxyisobutyryl)–OH: ^{1}H NMR (500 MHz, $CDCl_3$): δ 7.69 (d, J = 7.5 Hz, 2H), 7.54 (t, J = 7.5 Hz, 2H), 7.33 (t, J = 7.5 Hz, 2H), 7.23 (t, J = 7.5 Hz, 2H), 5.99 (d, J = 8.0 Hz, 1H), 4.30–4.40 (m, 3H), 4.12–4.14 (m, 1H), 3.18–3.19 (m, 2H), 1.64–1.84 (m, 2H), 1.37–1.47 (m, 10H); ^{13}C NMR (125 MHz, $CDCl_3$): δ 177.6, 174.9, 156.4, 143.7 (143.6), 141.2 (141.1), 127.7, 127.0, 125.0, 119.9, 73.5, 67.1, 53.6, 47.0, 38.6, 31.6, 28.7, 27.5 (27.4), 22.1; IR (KBr): 3361.7, 2934.8, 2868.3, 1711.2, 1696.9, 1642.5, 1631.6, 1536.4, 1454.6, 1270.5, 1254.9, 1200.1, 1176.6, 1047.3, 765.4, 740.3 cm^{-1}; HRMS (m/z): $[M]^{+}$ calcd. for C25H31N2O6, 455.2182; found, 455.2165.

Fmoc-Lys (4-(tritylO) butyryl)-OH.

Step 1. A mixture of 2.58 g (30 mmol, 2.28 ml) of 4-butyrolactone and 1.2 g (30 mmol) of sodium hydroxide in 30 ml of water was heated at 70 °C overnight. The clear solution was cooled and concentrated. The resulting white solid was suspended in toluene and concentrated further to remove the remaining trace amounts of water. An almost quantitative yield of sodium 4-hydroxybutyrate was obtained.

Step 2. Sodium 4-hydroxybutyrate (1.26 g, 10 mmol) and trityl chloride (10 mmol, 2.79 g) were dissolved in 30 ml pyridine for 3 d at 30 °C. The solvent was evaporated, and the residue was dissolved in ethyl ether. The ether solution was extracted with aqueous sodium hydroxide solution (4 g in 250 ml of H_2O). The aqueous solution was acidified to pH 3.0 and extracted twice with ethyl acetate. The combined organic phases were washed with brine and dried over anhydrous $MgSO_4$. The mixture was filtered, and the filtration was evaporated to dryness, giving the solid product 4-(tritylO) butyric acid (1.29 g, 37%).

Step 3. DCC (3.7 mmol, 760 mg) was added to a solution of 4-(tritylO) butyric acid (1.29 g, 3.7 mmol) and N-hydroxy-succinimide (3.7 mmol, 425 mg) in 30 ml dioxane .The reaction was stirred at room temperature for 10 h. The solution was filtered and evaporated to dryness, and then the residue was redissolved in 60 ml CH_2Cl_2. Et_3N (8 mmol, 1.2 ml) and Fmoc-Lys-OH (4 mmol, 1.62 g) were sequentially added. The mixture was stirred at room temperature for 4 h. After that, 150 ml water was added to the mixture, and the solution was adjusted to pH 2.3. The

organic layer was separated, and the aqueous layer was extracted with EtOAc. The combined organic layers were dried over anhydrous Na_2SO_4. The solvent was evaporated, and the residue was purified by flash column chromatography ($MeOH/CH_2Cl_2$ = 1:30). A yield of 1.5 g crude Fmoc-Lys (4-(tritylO) butyryl)-OH was obtained. The crude product contained more than 20% of 1, 3-dicyclohexylurea (DCU), as shown by MS results, but it was pure enough for peptide synthesis. Fmoc–Lys(4–tritylO butyryl)–OH: ^{1}H NMR (500 MHz, $CDCl_3$): δ 8.03 (s, 1H), 7.69–7.72 (m, 2H), 7.49–7.57 (m, 2H), 7.31–7.42 (m, 7H), 7.23–7.29 (m, 12H), 5.88 (t, J = 5.5 Hz, 1H), 5.83 (d, J = 8.5 Hz, 1H), 4.28–4.44 (m, 3H), 4.09–4.20 (m, 1H), 3.04–3.17 (m, 4H), 2.28 (t, J = 7.5 Hz, 2H), 1.67–1.94 (m, 4H), 1.26–1.39 (m, 4H); ^{13}C NMR (125 MHz, $CDCl_3$): δ 174.8, 174.0, 156.2, 144.1 (144.0), 143.9 (143.7), 141.2, 128.6 (128.5), 127.8 (127.7), 127.6, 127.03 (127.01), 127.98 (127.93), 125.15 (125.09), 119.9, 86.6, 67.0, 62.5, 53.6, 47.1, 39.0, 33.7, 31.7, 28.9, 26.0, 22.1; IR (KBr): 3420, 3325, 3059, 2934, 2869, 1718, 1653, 1539, 1492, 1449, 1419, 1336, 1265, 1221, 1073, 760, 740, 707 cm^{-1}; HRMS (m/z): $[M]^+$ calcd. for C44H45N2O6, 697.3278; found, 697.3268.

SUPPLEMENTAL REFERENCES

Anders, S., Pyl, P.T., and Huber, W. (2015). HTSeq--a Python framework to work with high-throughput sequencing data. Bioinformatics *31*, 166-169.

Chung, D.J., Zhang, Q., and Keles, S. (2014). MOSAiCS-HMM: A Model-Based Approach for Detecting Regions of Histone Modifications from ChIP-Seq Data. Front Probab Stat Sc, 277-295.

Dai, L.Z., Peng, C., Montellier, E., Lu, Z.K., Chen, Y., Ishii, H., Debernardi, A., Buchou, T., Rousseaux, S., Jin, F.L.*, et al.* (2014). Lysine 2-hydroxyisobutyrylation is a widely distributed active histone mark. Nat Chem Biol *10*, 365-U373.

Delaval, K., Govin, J., Cerqueira, F., Rousseaux, S., Khochbin, S., and Feil, R. (2007). Differential histone modifications mark mouse imprinting control regions during spermatogenesis. The EMBO journal *26*, 720-729.

Garcia, B.A., Mollah, S., Ueberheide, B.M., Busby, S.A., Muratore, T.L., Shabanowitz, J., and Hunt, D.F. (2007). Chemical derivatization of histones for facilitated analysis by mass spectrometry. Nature protocols *2*, 933-938.

Huang da, W., Sherman, B.T., and Lempicki, R.A. (2009a). Bioinformatics enrichment tools: paths toward the comprehensive functional analysis of large gene lists. Nucleic acids research *37*, 1-13.

Huang da, W., Sherman, B.T., and Lempicki, R.A. (2009b). Systematic and integrative analysis of large gene lists using DAVID bioinformatics resources. Nature protocols *4*, 44-57.

Kharchenko, P.V., Tolstorukov, M.Y., and Park, P.J. (2008). Design and analysis of ChIP-seq experiments for DNA-binding proteins. Nature biotechnology *26*, 1351-1359.

Kuan, P.F., Chung, D., Pan, G., Thomson, J.A., Stewart, R., and Keles, S. (2011). A Statistical Framework for the Analysis of ChIP-Seq Data. Journal of the American Statistical Association *106*, 891-903.

Landt, S.G., Marinov, G.K., Kundaje, A., Kheradpour, P., Pauli, F., Batzoglou, S., Bernstein, B.E., Bickel, P., Brown, J.B., Cayting, P.*, et al.* (2012). ChIP-seq guidelines and practices of the ENCODE and modENCODE consortia. Genome research *22*, 1813-1831.

Langmead, B., Trapnell, C., Pop, M., and Salzberg, S.L. (2009). Ultrafast and memory-efficient alignment of short DNA sequences to the human genome. Genome biology *10*, R25.

Liu, X., Sadhukhan, S., Sun, S., Wagner, G.R., Hirschey, M.D., Qi, L., Lin, H., and Locasale, J.W. (2015). High-Resolution Metabolomics with Acyl-CoA Profiling Reveals Widespread Remodeling in Response to Diet. Molecular & cellular proteomics : MCP *14*, 1489-1500.

Mootha, V.K., Lindgren, C.M., Eriksson, K.F., Subramanian, A., Sihag, S., Lehar, J., Puigserver, P., Carlsson, E., Ridderstrale, M., Laurila, E.*, et al.* (2003). PGC-1alpha-responsive genes involved in oxidative phosphorylation are coordinately downregulated in human diabetes. Nat Genet *34*, 267-273.
Robinson, M.D., and Smyth, G.K. (2007). Moderated statistical tests for assessing differences in tag abundance. Bioinformatics *23*, 2881-2887.
Robinson, M.D., and Smyth, G.K. (2008). Small-sample estimation of negative binomial dispersion, with applications to SAGE data. Biostatistics *9*, 321-332.
Shechter, D., Dormann, H.L., Allis, C.D., and Hake, S.B. (2007). Extraction, purification and analysis of histones. Nature protocols *2*, 1445-1457.
Subramanian, A., Tamayo, P., Mootha, V.K., Mukherjee, S., Ebert, B.L., Gillette, M.A., Paulovich, A., Pomeroy, S.L., Golub, T.R., Lander, E.S.*, et al.* (2005). Gene set enrichment analysis: a knowledge-based approach for interpreting genome-wide expression profiles. Proc Natl Acad Sci U S A *102*, 15545-15550.
Trapnell, C., Pachter, L., and Salzberg, S.L. (2009). TopHat: discovering splice junctions with RNA-Seq. Bioinformatics *25*, 1105-1111.
Zhang, Y., Liu, T., Meyer, C.A., Eeckhoute, J., Johnson, D.S., Bernstein, B.E., Nusbaum, C., Myers, R.M., Brown, M., Li, W.*, et al.* (2008). Model-based analysis of ChIP-Seq (MACS). Genome biology *9*, R137.